Short communication

Single and bimetallic catalyst screenings of noble metals for methane combustion

Weerit Kumsung[a], Metta Chareonpanich[a,b,c,d], Paisan Kongkachuichay[a,b,c,d], Selim Senkan[f], Anusorn Seubsai[a,b,c,e,*]

[a] Department of Chemical Engineering, Faculty of Engineering, Kasetsart University, Bangkok 10900, Thailand
[b] Center of Excellence on Petrochemical and Materials Technology, Kasetsart University, Bangkok 10900, Thailand
[c] NANOTEC Center for Nanoscale Materials Design for Green Nanotechnology, Kasetsart University, Bangkok 10900, Thailand
[d] Center for Advanced Studies in Nanotechnology and Its Applications in Chemical, Food and Agricultural Industries, Kasetsart University, Bangkok 10900, Thailand
[e] Center for Advanced Studies in Industrial Technology and Faculty of Engineering, Kasetsart University, Bangkok 10900, Thailand
[f] Department of Chemical and Biomolecular Engineering, University of California Los Angeles, Los Angeles, CA 90095, United States

ARTICLE INFO

ABSTRACT

Single metals and bimetallics impregnated on γ-Al_2O_3 were screened for methane combustion. A screening of 20 noble metals was first performed in a fuel-rich condition, revealing the top six active metals: Rh, Ru, Pd, Pt, Cu, and Cr, in order of decreasing activity. Then, the screening of the combinations of these six metals delivered several catalysts that offered a higher methane conversion when compared to the most active single catalysts. (4 wt% Rh + 1 wt% Cr)/γ-Al_2O_3 achieved the highest methane combustion and provided excellent stability. NH_3-TPD analysis revealed strong acid sites playing a key role in the activation of methane.

1. Introduction

In freezing-cold places, houses need a heater to keep the temperature warm. Such heaters can be classified into two types: that are namely; electrical heater and gas catalytic heater. For the latter, the heat is generated by the combustion of fuel gases such as methane (CH_4) and propane, with combustion of the fuel gases in air occurring in a catalytic pad. The products from the combustion are CO_2, CO, and H_2O, depending on the processes of combustion: (1) complete or (2) incomplete combustions. Reaction equations for CH_4 combustion are as follows:

$$CH_4 + 2O_2 \rightarrow CO_2 + 2H_2O; \quad \text{complete combustion} \quad (1)$$

$$2CH_4 + 3O_2 \rightarrow 2CO + 4H_2O; \quad \text{incomplete combustion} \quad (2)$$

Generally, Pt catalyst ceramic composite is commercially used for this operation. However due to the high cost of Pt, the fact that it has poor-stability at high reaction temperatures [1], and the fact that it has lower activity compared to some other catalysts [2–4], the new development of new economical and highly active catalysts for the combustion process is essential.

Various catalysts in CH_4 combustion have been explored to achieve better activity and higher catalytic stability. These catalysts are mostly from transition metals such as Pt, Rh, and Pd. In a study of these three

metals impregnated on γ-Al_2O_3 under a fuel-rich condition, the CH_4 conversions of Pd and Rh catalysts were found to be higher than those of Pt catalyst in a temperature range of 300–800 °C [2]. In other work, Pd and Rh were mixed and embedded on γ-Al_2O_3, giving a CH_4 conversion of 87% at 550 °C. The addition of Pd 1 wt% to the Rh catalyst could improve the activity when compared to the single Pd or Rh catalysts, because the formation of Rh_2O_3 inhibited the reduction of PdO to Pd(0) and thus the Pd oxide form enhanced combustion of CH_4 [5]. When Pd and Rh were combined and embedded on a metal-foam support, a CH_4 conversion of 96.7% was attained and a stability test at atmospheric pressure and 750 °C for 200 h showed a steady CH_4 conversion [6]. In a similar study of Rh impregnated on ZrO_2, a CH_4 conversion of 60% was achieved at 600 °C. This study suggested that the metallic dispersion and oxidation state of Rh improved the catalytic activity of CH_4 combustion [7]. Rh was also used with $LaMnO_3$/Al_2O_3 support; approximately 90% CH_4 conversion and 80% CO selectivity were achieved at 600 °C. The manganese from $LaMnO_3$/Al_2O_3 support was found to reduce the light-off temperature, while the perovskite was found to improve the stability of Rh particles [8]. In other research, Cr catalyst for CH_4 combustion has been studied due to its low cost. In a study wherein Cr catalyst was used with Ce added by wet impregnation, Cr-based catalyst with 3 wt% of Ce was the most active catalyst, giving 70% conversion CH_4 at 400 °C [9]. Finally in some recent works, three-

---

dimensionally-ordered macroporous (3DOM) materials possessing a high surface area were synthesized and were found to deliver an improvement in CH_4 combustion [10]. Among these materials are 1D single-crystalline perovskite [11], 3DOM perovskites [12], Pt nanoparticles on 3DOM $Ce_{0.6}Zr_{0.3}Y_{0.1}O_2$ [13], and Ag on 3DOM $La_{0.6}Sr_{0.4}MnO_3$ [14], all of which have been become increasingly of interest in the field.

Although there have been several noble metal catalysts investigated for used in CH_4 combustion, tests of the above-mentioned single metal catalysts have never been reported in terms of catalyst activity under the same testing conditions. Furthermore, bimetallic catalysts of those single noble metals have never been systematically explored and identified for CH_4 combustion. Herein, we used a combinatorial approach [15,16] to explore the top-most active single and bimetallic catalysts for CH_4 combustion from 20 selected noble elements. The most active catalyst was then characterized to understand its physicochemical properties in relation to the catalyst performance.

2. Experimental

2.1. Catalyst preparation

Single and bimetallic catalysts were prepared by impregnation. In brief, the catalysts were prepared as follows. 20 metal precursors (see Table S1) were dissolved in DI water as a stock solution. First, each stock solution was determined and pipetted into commercial γ-Al_2O_3 (Alfa Aesar, 99.97%, 3 μm APS powder) to achieve 5 wt% of single noble metal supported on γ-Al_2O_3. The solution was stirred at room temperature for 1 h, then heated to 170 °C and stirred until dried. A fine powder obtained was taken to calcine at 750 °C for 6 h. Second, the bimetallic catalysts were prepared by selecting the six elements showing the highest CH_4 conversion from the catalyst screening of the single catalysts. Five metal ratios were examined for each pair and the total metal loading of each pair, loaded on γ-Al_2O_3 was 5 wt%, i.e. 5 wt% A + 0 wt% B, 4 wt% A + 1 wt% B, …, 0 wt% A + 5 wt% B, where A and B are each selected elements. The impregnation, drying, and calcination procedures were the same as for the preparation of the single catalysts.

2.2. Catalyst characterization

X-ray powder diffraction (PXRD, Bruker AXS/Diffraktometer D8) was used to determine crystallization of the catalysts. The operating parameters were monochromatic Cu–K_α radiation, 40 kV, 40 mA, a step size of 0.02°, and a scan speed of 0.5 s/step. N_2 physisorption using a Quantachrome Autosorp-1C instrument with BET method at −196 °C was used to determine the specific surface area of samples. Elemental compositions of the samples were analyzed by using a scanning electron microscope with an energy dispersive X-ray spectrometer (FE-SEM/EDX, FE-SEM: JEOL JSM7600F). Ammonia-temperature programmed desorption (NH$_3$-TPD) was used to determine the acidic sites of the catalysts (Thermofinnigan model 1100). 0.25 g of the catalyst was pretreated under N_2 flow at 400 °C for 1 h and cooled down to 40 °C before 10% NH_3/He mixed gas was flowed over the catalysts for 30 min to adsorb on the acid sites. The excess ammonia was eradicated by flowing N_2 at 40 °C for 30 min. Then the catalysts were heated to 800 °C at a heating rate of 10 °C/min, while He was passed over the catalysts at 30 mL/min. All of the gas flow rates in each step were 30 mL/min.

2.3. Catalytic activity test

A sketch of the testing system is shown in Fig. S1. 10 mg of each prepared catalyst was packed in a quartz tube reactor (0.5 cm inner diameter) and sandwiched between layers of quartz wool. If not otherwise indicated, the reactor temperature was set at 475 °C and atmospheric pressure was used. After the reactor temperature reached the setting point, the tubular reactor containing the catalyst was introduced into the reactor system. Then, a feed gas containing O_2 (37.5%) and CH_4 (62.5%) at a volume ratio of $O_2/CH_4 = 28.0/46.7$, and without any inert gas, was introduced into the tubular reactor at a total feed flow rate of 5 mL/min, corresponding to a gas hourly space velocity (GHSV) of 15,000 h^{-1}. It should be noted that the fuel-rich condition was investigated in this work because the condition can better approximate or simulate the situation of the fuel gas meeting the catalytic pad when using a catalytic heater. Mass flow controllers (KOFLOC 3810 DSII) were used to control all of the feed gas flow rates in the system. The system was left to sit for 1 h without any catalyst pretreatment or activation prior to sampling the effluent gas. Gas chromatography was an online Gas Chromatograph (SHIMADZU, GC-14A) equipped with a thermal conductivity detector (TCD). The detected products were CO, CO_2, and H_2O. Some catalysts also produced a trace amount of H_2. The activity of the catalyst was evaluated after the system was left at the setting condition for 1 h and was determined using the amount of the CH_4 conversion, CO_2 selectivity, and CO selectivity, as expressed in Eqs. (3), (4), and (5), respectively:

$$\%CH_4\ conversion = 100 \times \frac{moles\ of\ CO_2 + moles\ of\ CO}{moles\ of\ CO_2 + moles\ of\ CO + moles\ of\ CH_4\ left} \tag{3}$$

$$\%CO_2\ selectivity = 100 \times \frac{moles\ of\ CO_2}{moles\ of\ CO_2 + moles\ of\ CO} \tag{4}$$

$$\%CO\ selectivity = 100 \times \frac{moles\ of\ CO}{moles\ of\ CO_2 + moles\ of\ CO} \tag{5}$$

3. Results and discussion

Fig. 1 presents the CH_4 conversions using 5 wt% of the single catalysts; results fall in a range of 0.1–11.4%. The top six active catalysts were (in order) 5Rh > 5Ru > 5Pd > 5Pt > 5Cu > 5Cr, yielding 11.4–4.6% CH_4 conversion. The other catalysts provided CH_4 conversions of < 2.5%. Our results are in a good agreement with experiments done by Lyubovsky et al., in which the single catalysts of Pd, Pt, or Rh on γ-Al_2O_3 were used for CH_4 combustion; this work found that in a fuel-rich condition ($O_2/CH_4 = 2/3$ by volume) and at constant temperature (475 °C), Rh catalyst showed the highest activity for the combustion products, followed by the Pd and Pt catalysts. When the reaction temperature was varied, the Rh and Pd catalysts had a light-off temperature of 400 °C, lower than that of the Pt catalyst at 500 °C [2]. Similarly, Hickman et al. found that Rh-coated monolith had an
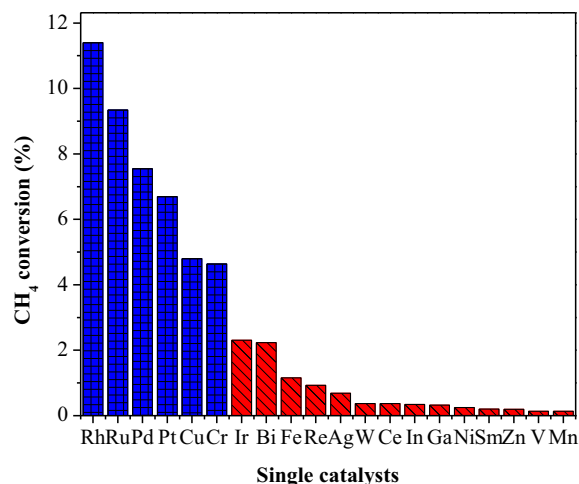
Fig. 1. CH_4 conversion of γ-Al_2O_3-supported single catalysts.

activation energy less than that of Pt-coated monolith catalyst [17]. Another study of CH_4 reaction for Ru, Rh, and Pt catalysts supported on Al_2O_3 showed that, at 500 °C, the highest CH_4 conversion was obtained for the Rh/Al_2O_3 catalyst, followed by Ru and Pt catalysts. The Rh catalyst achieved complete CH_4 conversion (i.e. 100 %) at 660 °C, while the Ru and the Pt catalysts achieved complete CH_4 conversion at 699 °C and over 800 °C, respectively [4]. Reactions with the other metals presented in Fig. 1 have not been reported under this fuel-rich condition. However, some transition metals including Co, Mn, Cr, Cu, and Ni supported on Al_2O_3 were investigated by Paredes et al. under a fuel-lean condition; they found that the catalytic activity at 550 °C was ranked as follows: Co > Mn > Cr > Cu > Ni [18], results which differ from our findings due to the difference in the fuel composition. Discussion of activity in relation to the catalyst properties will be presented later in this paper.

The top six active single metals that achieved the highest % CH_4 combustion (i.e. Rh, Ru, Pd, Pt, Cu, and Cr) were chosen for the preparation of bimetallic catalysts, which were made by combining each one with the other five in turn. Each pair of the metal combinations was prepared at 5 different metal ratios, and the total metal loading of each one was fixed at 5 wt%. Fig. 2 shows the % CH_4 conversions of all possible bimetallic catalysts. The % CH_4 conversions were in the range of 0.1%–15.9%, and the average was 8.9%. This clearly showed that the activity of several bimetallic catalysts was much higher than that of the top six single catalysts. 17 of these bimetallic catalysts achieved a CH_4 conversion > 11.4% and gave an activity for CH_4 combustion higher than of the single Rh catalyst (the single catalyst with the highest conversion). The maximum CH_4 conversion was obtained using the combination of 4 wt% Rh and 1 wt% Cr (4Rh1Cr): 15.9%, that is, approximately 1.4 or 3.4 times the conversion of the single Rh and Cr catalysts, respectively. Note that when the repeatability of the best five active bimetallic catalysts was also investigated by performing the testing procedure for each chosen catalyst in tuplicate, standard deviations were found in a range of 0.03–0.53 (see Table S2).

In a previous study of CO_2 reforming of CH_4 over Ni-Cr/yttria-doped ceria catalysts, the role of Cr was suggested to be in the enhancement of the metallic dispersion and provision of surface oxygen vacancies on the catalyst, and thus the promotion of CH_4 combustion [19]. In addition, Cr was found to reduce the light-off temperature of the reaction, which implies that the products were easily generated at lower reaction temperatures [20]. Pecchi et al. studied CH_4 combustion using Rh/ZrO_2 and found that the Rh^+ state and the metallic dispersion of the catalyst played a key role in the improvement of the activity for CH_4 combustion [7]. These studies imply that the physicochemical properties of the Rh and Cr components support each other, explaining why the best activity for CH_4 conversion in this work is given by 4Rh1Cr. The 4Rh1Cr catalyst exhibits a synergistic catalyst effect, which will be discussed in the analysis of catalysts using NH_3-TPD.

Furthermore, the effect of varying the reactor temperature used with 4Rh1Cr, 5Rh, and 5Cr catalysts was investigated (see Fig. S2). Note that the possible maximum CH_4 conversion in theory under this condition was 40.0%. As observed, at each temperature, the 5Cr catalyst achieved the lowest CH_4 conversion. Above 400 °C, the 4Rh1Cr catalyst evidently gave CH_4 conversions higher than those of the 5Rh catalyst. The light-off temperature of the 4Rh1Cr catalyst was established at approximately 545 °C, about 37 °C lower than that of the 5Rh catalyst. For the 5Cr catalyst, CH_4 conversion slowly increased and the light-off temperature was not clear. When increasing the of O_2/CH_4 feed gas ratio from 0.6–2.0 with a constant total feed flow rate of 5 mL/min (see Fig. S3), CH_4 conversion and CO_2 selectivity sharply increased to nearly 100% at a O_2/CH_4 feed gas ratio of 2.0, while the CO selectivity decreased to 0%. This suggests that complete combustion can occur in an excess supply of O_2, i.e. O_2/CH_4 feed gas ratio > 2.0.

Fig. 3 shows PXRD patterns of the single 5Rh, 5Cr, and bimetallic 4Rh1Cr catalysts. The γ-Al_2O_3 support shows diffraction peaks at 33.7, 36.3, 45.8, 61.7, and 67.3 (ICDD 00-010-0425) appearing for all catalysts. In particular, the diffraction peaks at 19.2 and 54.3 (ICDD 00-041-0541) were assigned to the Rh_2O_3 component in the 5Rh and 4Rh1Cr catalysts. It seems that the diffraction peaks of the Cr component (i.e. Cr_2O_3) in the 5Cr and 4Rh1Cr catalysts were undetectable because Cr might be in the amorphous phase. In addition after being used for 1 h, the three catalysts were taken to be analyzed by PXRD. Interestingly, the peak intensities of Rh_2O_3 in 4Rh1Cr and 5 Rh catalysts were found to decrease, and two new peaks at $2\theta = 41.0$ and 48.0 (ICDD 00-005-0685), indicating the presence of the Ru(0), appeared. Similarly, the Ru(0) phase was also seen in the 4Rh1Cr catalyst used for 8 h. For 5Cr catalyst, no clear PXRD peaks of Cr(0) were observed. This agrees with a study of oxidative dehydrogenation of isobutene to isobutene under a fuel-rich condition, wherein it was found that Cr^{3+} (i.e. Cr_2O_3) species was dominant during the reaction [21]. The preceding results can imply that the Rh(0) phase is the co-active component with Cr_2O_3 during the reaction.

The BET surface areas of the 5Rh, 5Cr, and 4Rh1Cr catalysts were measured and found to be 70, 57, and 58 m^2/g, respectively, which were slightly lower than that of the γ-Al_2O_3 support (80 m^2/g), as a

	Cr	Cu	Pt	Pd	Ru	Rh
5X	4.6	4.8	6.7	7.6	9.3	11.4
4X + 1Rh	10.6	4.1	13.0	12.3	9.0	
3X + 2Rh	13.8	3.6	13.2	14.9	12.3	
2X + 3Rh	15.1	11.2	14.4	13.4	11.8	
1X + 4Rh	15.9	11.3	12.3	14.0	13.0	
4X + 1Ru	9.7	7.4	9.2	12.0		
3X + 2Ru	8.3	7.2	9.1	12.1		
2X + 3Ru	10.5	8.1	11.0	1.8		
1X + 4Ru	8.6	7.1	6.3	8.5		
4X + 1Pd	0.1	3.7	12.0			
3X + 2Pd	9.1	7.9	6.9			
2X + 3Pd	1.9	9.0	7.4			
1X + 4Pd	13.9	7.7	9.9			
4X + 1Pt	5.9	3.4				
3X + 2Pt	7.9	8.7				
2X + 3Pt	5.6	4.9				
1X + 4Pt	9.1	4.4				
4X +1 Cu	4.3					
3X + 2Cu	5.0					
2X + 3Cu	8.1					
1X + 4Cu	2.6					

>14.1

12.1 - 14.0

10.1 - 12.0

8.1 - 10.0

<8.0

Fig. 2. CH_4 conversion for γ-Al_2O_3-supported bimetallic catalysts, showing all the combinations of Rh, Ru, Pd, Pt, Cu, and Cr. The total metal loading was fixed at 5 wt%.
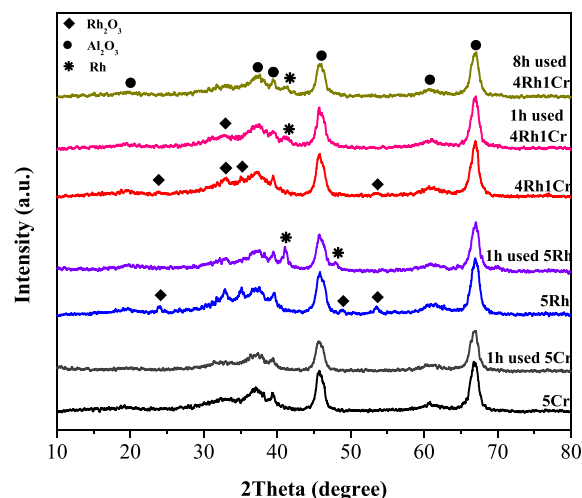
Fig. 3. XRD patterns of fresh and used catalysts: 5Rh, 5Cr, and 4Rh1Cr.
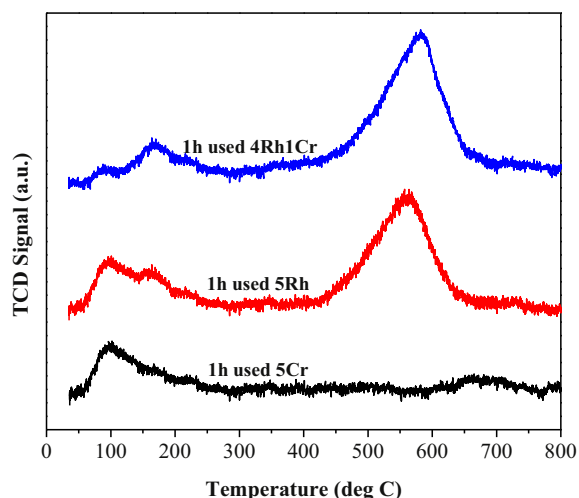
Fig. 4. NH$_3$-TPD profiles of catalysts: 5Rh, 5Cr, and 4Rh1Cr after used for 1 h.

Fig. 5. Time-on-stream testing results of 4Rh1Cr catalyst over 97 h.

result of the preparation effects (i.e. calcination temperature, metal loading). The elemental compositions of these three catalysts were also determined by SEM/EDX, giving results in a good agreement with theoretical values (see Table S3). Moreover, Rh$_2$O$_3$ nanoparticles with an average size of 17 nm for both 4Rh1Cr and 5Rh catalysts were found using TEM images (see Figs. S4–S5). Again, Cr$_2$O$_3$ crystals could not be seen in the TEM images because they were in the amorphous phase and could not be distinguished from the support (see Fig. S6).

Fig. 4 shows NH$_3$-TPD spectra and thus the acidity of the 5Rh, 5Cr, and 4Rh1Cr catalysts after being used for 1 h. Each peak area of the catalysts is quantified as presented in Table S4. For all catalysts, there were some weak-intensity peaks of around 50–250 °C, which were assigned to the NH$_3$ desorption from weak acidic sites. The 5Rh and 4Rh1Cr catalysts had a similar peak at about 400–650 °C, which was assigned to NH$_3$ desorption of the strong acidic sites. Meanwhile, the strong acidic sites of the 5Cr catalyst did not appear. Interestingly, with the addition of Cr, the strong acidic sites of the 5Rh catalyst at 560 °C shifted toward a higher temperature (585 °C). Moreover, the 4Rh1Cr/5Rh peak area ratio of the strong acidic sites was 1.43. These results indicate that the strong acidic sites play an important role in the combustion of CH$_4$, and a higher number of strong acidic sites results in an increase in the catalytic activity for CH$_4$ combustion.

Generally, CH$_4$ molecules do not easily absorb on a solid surface and continue to react unless the surface possesses highly active sites to accommodate them. In a study by Lu et al. on the role of acidity of Pd/ZSM-5 catalyst in CH$_4$ combustion, the presence of a great amount of Brønsted acid sites, referring to the acidic hydroxyl species attached to the ZSM-5 supports, strongly influenced the catalytic activity for CH$_4$ activation [22]. Some other studies have also suggested that an increase of the acidity of catalyst surface favors the breaking of C−H bonds in CH$_4$ molecules [23–25]. These studies can potentially be applied to our 4Rh1Cr catalyst, over which the CH$_4$ is activated by the Brønsted acid sites (i.e. strong acid sites) where the oxygen species attach to the proton. After CH$_4$ is adsorbed by oxygen, the two together can further create CO$_x$ and H$_2$O [26]. The absorbed oxygen species, which could be a part of either the active metal oxides [27] or the active metal oxides promoted by supports [28], must desorb from the surface as CO$_x$, such that oxygen vacancies on the catalyst surface are created and subsequently refilled with the feed gas oxygen [29]. A new cycle then occurs. The identification of active sites, as well as the mechanism, needs further study.

Since the catalyst stability is important, a time-on-stream experiment of the 4Rh1Cr catalyst was performed. Fig. 5 charts CH$_4$ conversion, CO selectivity, and CO$_2$ selectivity over 97 h of continuous operation at 475 °C and a O$_2$/CH$_4$ ratio of 28.0/46.7 by volume. As
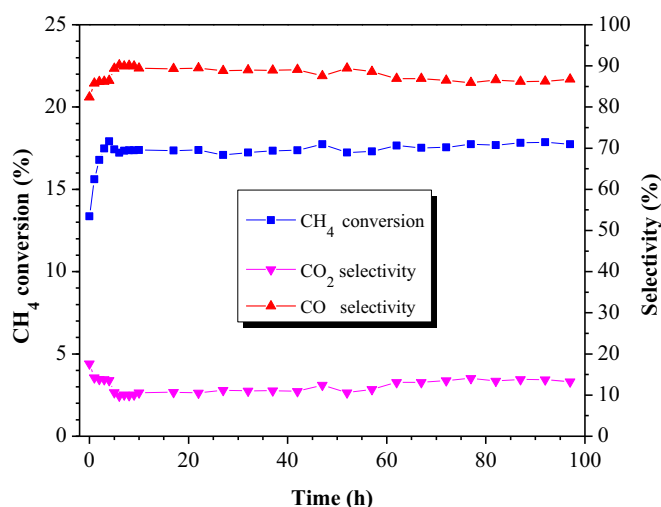
indicated in the figure, the CO selectivity is much higher than the CO$_2$ selectivity; this is because the production of CO is normally favored under the fuel-rich condition, owing to there being insufficient oxygen for complete combustion. In these experiments, the CH$_4$ conversion gradually increased for the first 2 h, and then remained steady at approximately 17%. Likewise, CO and CO$_2$ selectivities were virtually constant during hours 3–97: 86% and 14%, respectively. Note that a trace amount of H$_2$ (< 1.0% selectivity) was also found in the effluent gas analysis by GC, suggesting that coke formation could have occurred. However, observing the quartz tubular reactor, no black film was seen on the wall after the 97-h experiment (see Fig. S7) and the catalyst stability was excellent within the time period. These latter findings implied that carbonaceous materials did not deposit on the catalyst's surface. This implies that the 4Rh1Cr catalyst is quite durable for the reaction. When comparing this catalyst to the other catalysts (see Table S5), it can be established that 4Rh1Cr is a catalyst of high activity at low reactor temperature.

4. Conclusion

The top six active noble metals supported on γ-Al$_2$O$_3$–Rh, Ru, Pd, Pt, Cu, and Cr– were achieved from the single catalyst screening. A bimetallic catalyst screening from the combinations of these six metals later led to the discovery of several bimetallic catalysts that were more active than the commercial Pt/γ-Al$_2$O$_3$ catalyst. Among these, the greatest activity was attained by the 4Rh1Cr catalyst because of the increase in the strong acid sites on this catalyst's surface, which enhanced the activation of C−H bonds in CH$_4$. Moreover, in monitoring the activity over 97 h, the 4Rh1Cr catalyst was found to be quite stable, which means that it can potentially be considered for commercial use.

Appendix A. Supplementary data

Supplementary data to this article can be found online at https://doi.org/10.1016/j.catcom.2018.03.022.

References

[1] M. Bosomoiu, G. Bozga, G. Soare, Methane combustion over a commercial platinum on alumina catalyst: kinetics catalyst deactivation, Rev. Roum. Chim. 53 (2008) 1105–1115.

[2] M. Lyubovsky, L.L. Smith, M. Castaldi, H. Karim, B. Nentwick, S. Etemad, R. LaPierre, W.C. Pfefferle, Catalytic combustion over platinum group catalysts: fuel-lean versus fuel-rich operation, Catal. Today 83 (2003) 71–84.

[3] N. Kraikul, S. Jitkarnka, A. Luengnaruemitchai, Catalytic methane combustion on Pd-Pt-La catalysts and their surface models, Appl. Catal. B. 58 (2005) 143–152.

[4] U.E.S. Amjad, A. Vita, C. Galletti, L. Pino, S. Specchia, Comparative study on steam and oxidative steam reforming of methane with noble metal catalysts, Ind. Eng. Chem. Res. 52 (2013) 15428–15436.

[5] A. Maione, F. André, P. Ruiz, The effect of Rh addition on Pd/γ-Al2O3 catalysts deposited on FeCrAlloy fibers for total combustion of methane, Appl. Catal. A. 333 (2007) 1–10.

[6] P.S. Roy, N.K. Park, K. Kim, Metal foam-supported Pd–Rh catalyst for steam methane reforming and its application to SOFC fuel processing, Int. J. Hydrog. Energy 39 (2014) 4299–4310.

[7] G. Pecchi, P. Reyes, R. Gómez, T. López, J.L.G. Fierro, Methane combustion on Rh/ZrO2 catalysts, Appl. Catal. B. 17 (1998) L7–L13.

[8] S. Cimino, G. Landi, L. Lisi, G. Russo, Rh-La(Mn,co)O3 monolithic catalysts for the combustion of methane under fuel-rich conditions, Catal. Today 117 (2006) 454–461.

[9] X. Yuan, S. Chen, H. Chen, Y. Zhang, Effect of Ce addition on Cr/γ-Al2O3 catalysts for methane catalytic combustion, Catal. Commun. 35 (2013) 36–39.

[10] J. Chen, H. Arandiyan, X. Gao, J. Li, Recent advances in catalysts for methane combustion, Catal. Surv. Jpn. 19 (2015) 140–171.

[11] H. Arandiyan, H. Chang, C. Liu, Y. Peng, J. Li, Dextrose-aided hydrothermal preparation with large surface area on 1D single-crystalline perovskite La0.5Sr0.5CoO3 nanowires without template: highly catalytic activity for methane combustion, J. Mol. Catal. A 378 (2013) 299–306.

[12] H. Arandiyan, J. Scott, Y. Wang, H. Dai, H. Sun, R. Amal, Meso-molding three-dimensional macroporous perovskites: a new approach to generate high-performance nanohybrid catalysts, ACS Appl. Mater. Interfaces 8 (2016) 2457–2463.

[13] H. Arandiyan, H. Dai, K. Ji, H. Sun, Y. Zhao, J. Li, Enhanced catalytic efficiency of Pt nanoparticles supported on 3D ordered macro-/mesoporous Ce0.6Zr0.3Y0.1O2 for methane combustion, Small 11 (2015) 2366–2371.

[14] H. Arandiyan, H. Dai, J. Deng, Y. Wang, S. Xie, J. Li, Dual-templating synthesis of three-dimensionally ordered macroporous La0.6Sr0.4MnO3-supported Ag nanoparticles: controllable alignments and super performance for the catalytic combustion of methane, Chem. Commun. 49 (2013) 10748–10750.

[15] D. Zhang, L. Zhang, B. Liang, Y. Li, Effect of acid treatment on the high-temperature surface oxidation behavior of FeCrAlloy foil used for methane combustion catalyst support, Ind. Eng. Chem. Res. 48 (2009) 5117–5122.

[16] M. Kahn, A. Seubsai, I. Onal, S. Senkan, High throughput synthesis and screening of new catalytic materials for the direct epoxidation of propylene, Comb. Chem. High Throughput Screen. 13 (2010) 67–74.

[17] D.A. Hickman, L.D. Schmidt, Synthesis gas formation by direct oxidation of methane over monoliths, in: M.J. Comstock (Ed.), Catalytic Selective Oxidation, American Chemical Society, 1993, pp. 416–426.

[18] J.R. Paredes, E. Díaz, F.V. Díezet, S. Ordóñez, Combustion of methane in lean mixtures over bulk transition-metal oxides: evaluation of the activity and self-deactivation, Energy Fuel 23 (2009) 86–93.

[19] J.B. Wang, L.E. Kuo, T.J. Huang, Study of carbon dioxide reforming of methane over bimetallic Ni-Cr/yttria-doped ceria catalysts, Appl. Catal. A. 249 (2003) 93–105.

[20] Y. Liu, S. Wang, D. Gao, T. Sun, C. Zhang, S. Wang, Influence of metal oxides on the performance of Pd/Al2O3 catalysts for methane combustion under lean-fuel conditions, Fuel Process. Technol. 111 (2013) 55–61.

[21] S.M. Al-Zahrani, N.O. Elbashir, A.E. Abasaeed, M. Abdulwahed, Catalytic performance of chromium oxide supported on Al2O3 in oxidative dehydrogenation of isobutane to isobutene, Ind. Eng. Chem. Res. 40 (2001) 781–784.

[22] O. M'Ramadj, D. Li, X. Wang, B. Zhang, G. Lu, Role of acidity of catalysts on methane combustion over Pd/ZSM-5, Catal. Commun. 8 (2007) 880–884.

[23] Y. Wang, H. Arandiyan, J. Scott, M. Akia, H. Dai, J. Deng, K.F. Aguey-Zinsou, R. Amal, High performance Au–Pd supported on 3D hybrid strontium-substituted lanthanum manganite perovskite catalyst for methane combustion, ACS Catal. 6 (2016) 6935–6947.

[24] W. Fu, X.H. Li, H.L. Bao, K.X. Wang, X. Wei, Y.Y. Cai, J.S. Chen, Synergistic effect of Brønsted acid and platinum on purification of automobile exhaust gases, Sci. Rep. 3 (2013) 2349.

[25] W. Wang, M. Hunger, Reactivity of surface alkoxy species on acidic zeolite catalysts, Acc. Chem. Res. 41 (2008) 895–904.

[26] R.A. Dalla Betta, D.G. Löffler, Selectivity considerations in methane catalytic combustion, in: B.K. Warren, S.T. Oyama (Eds.), Heterogeneous Hydrocarbon Oxidation, American Chemical Society, 1996, pp. 36–47.

[27] Z. Zhao, B. Wang, J. Ma, W. Zhan, L. Wang, Y. Guo, Y. Guo, G. Lu, Catalytic combustion of methane over Pd/SnO2 catalysts, Chin. J. Catal. 38 (2017) 1322–1329.

[28] W.R. Schwartz, L.D. Pfefferle, Combustion of methane over palladium-based catalysts: support interactions, J. Phys. Chem. C 116 (2012) 8571–8578.

[29] Q. zafar, A. Abad, T. Mattisson, B. Gevert, M. Strand, Reduction and oxidation kinetics of Mn3O4/Mg–ZrO2 oxygen carrier particles for chemical-looping combustion, Chem. Eng. Sci. 62 (2007) 6556–6567.